MECHANISM OF ALUMINUM CARBIDE FORMATION IN ALUMINUM ELECTROLYSIS CELLS

Y.-W. Wang *, P.-C. Hao, J.-P. Peng, Y.-Z. Di

School of Metallurgy, Northeastern University, Shenyang, Liaoning, China

Abstract

The formation and dissolution of aluminum carbide is considered the primary factor affecting the life of aluminum electrolysis cells. Herein, the characteristics of sodium-graphite intercalation compounds (Na-GICs) were measured and the formation mechanism of Al_4C_3 during the aluminum electrolysis process was experimentally studied. The Na-GIC characteristics and the products of aluminum and Na-GIC reactions were investigated by Raman spectroscopy, X-ray diffraction, X-ray photoelectron spectroscopy, and scanning electron microscopy. The results showed that graphite can react with the sodium metal to form Na-GICs, which were detectable by Raman spectroscopy. Sodium inserted into the graphite layered structure acted as an intercalation agent to change the original graphite layered structure and increase the volume and specific surface area of graphite. Further, Al_4C_3 was produced by using sodium-graphite intercalation compounds and aluminum as materials. Thus, the presence of sodium plays an important role in the formation process of Al_4C_3 in aluminum electrolysis cells.

Keywords: Aluminum carbide; Aluminum electrolysis cells; Sodium-penetrated; Graphite; Formation mechanism

1. Introduction

In recent years, there has been increasing interest in the lifetime of aluminum reduction cells because of the rapidly developing aluminum reduction industry. One of the most common reasons for failure of aluminum cells is the wear of the cathode carbon block caused primarily by physical abrasion and chemical wear [1]. The chemical wear is mainly caused by formation and dissolution of Al_4C_3 [2]. The yellow Al_4C_3 can be observed in these aluminum cells on the exposed carbon surfaces and in cracks and gaps, and a 0.5-2 cm thick layer of Al_4C_3 also forms underneath the cathode carbon blocks. With the rapid increase of physical abrasion resistance of graphitized cathodes, chemical erosion is thought to be a stronger wear process [3].

Generally, molten aluminum infiltrating from the aluminum reduction bath may react directly with the carbon cathode to form aluminum carbide according to the reaction:

$$4Al(l) + 3C(s) = Al_4C_3(s) \qquad (1)$$
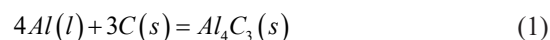
This reaction is thermodynamically favored at all temperatures of concern in the electrolytic aluminum production ($\Delta G^\theta = -147$ kJ (970°C)) [4]. However, evidence suggests that the molten aluminum and carbon cathode cannot react with each other below 1000°C [5]. Two key factors influence the reaction between molten aluminum and the carbon cathode; where one is thermodynamics and the other is the wettability of the system. Typically, contact between liquid aluminum and carbon does not induce appreciable carbide formation, but the reaction is enhanced by the presence of cryolite or a cryolite-containing melt. It is generally accepted that the formation of Al_4C_3 by electrolysis may be chemical (Eqn. (2)) or electrochemical (Eqn. (3)) in the presence of cryolite or a cryolite-containing melt [6, 7], such that:

$$Anodic: \ 4Al(l) + 12F^-(diss) = 4AlF_3(diss) + 12e^- \qquad (2)$$

$$Cathodic: \ 3C(s) + 4AlF_3(diss) + 12e^- =$$
$$Al_4C_3(s) + 12F^-(diss) \qquad (3)$$
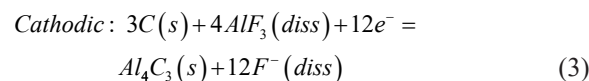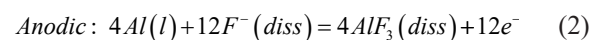
However, no electrochemical reaction is present in the cracks, gaps, and underneath the cathode carbon blocks. Instead, the action of cryolite is likely to serve as a wetting agent and as a solvent of oxide films, metallic aluminum, and the initial aluminum carbide product. Further, some researchers believe that the

presence of sodium in the carbon cathode blocks plays an important role in the formation process of Al_4C_3. Bonadia [8] posited that aluminum carbide was formed by the reaction of cryolite with sodium and carbon (Eqn. (4)). Solheim et al. [9] found a large amount of NaF in the spent carbon cathode blocks, and considered that the increase of molecular ratio of penetrated electrolyte resulted in the formation of Al_4C_3. This Al_4C_3 was formed by the reaction between C and AlF_3 (Eqn. (5)). These reactions are given as:

$$4Na_3AlF_6 + 12Na + 3C = Al_4C_3 + 24NaF \qquad (4)$$

$$4AlF_3 + 12Na + 3C = Al_4C_3 + 12NaF \qquad (5)$$
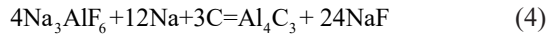
In actuality, experimental studies show that Al_4C_3 can also be produced by reacting aluminum and carbon blocks in the presence of NaF or Na metal [10]. It seems that the presence of sodium is a key point for the formation process of Al_4C_3 in aluminum electrolysis cells.

In the present work, the form of sodium existing in graphite blocks and the formation mechanism of aluminum carbide in the presence of sodium were studied.

2. Experimental

During the aluminum electrolysis process, sodium penetration occurs by both pore penetration and crystal lattice diffusion, where the latter is the primary mechanism of sodium penetration [11,12]. Some researchers believe that most of the penetrated sodium in the carbon cathode block is in the form of Na_xC intercalation compounds [13].

Herein, sodium-penetrated graphite was initially produced. For this, sodium metal was produced by aluminothermic reduction firstly. In the sodium metal production process, a mixture of aluminum powder and NaF powder was pressed into pellets and NaF in the pellets was reduced to metal sodium in a horizontal retort with external heating under vacuum condition at 920°C. The sodium metal was collected on a condenser located in the cold side of retort. The sodium metal on the condenser was cut and put into a pure corundum crucible with an inside diameter of 50 mm, and an outside diameter of 70 mm and a height of 150 mm in the glove box. Then the sodium was covered by graphite powder. The mass ratio of graphite powder and sodium metal is 20:1. The pure corundum crucible with a cover was buried in graphite powder with a covering layer of over 50 mm, which effectively excluded air from the crucible. Finally, the corundum crucible was heated and kept at 920°C for 2 h, after which the sodium-penetrated graphite was obtained.

Next, the sodium-penetrated graphite was removed from the corundum crucible and a portion was mixed with pure aluminum powder. This sodium-penetrated graphite/aluminum mixture was subsequently placed in another pure corundum crucible with a cover and buried in graphite powder. These operations were performed in air. The corundum crucible was then heated and kept at 920°C for 2 h, whereupon the final product was obtained after the corundum crucible was reduced to room temperature.

The sodium-penetrated graphite was characterized by Raman spectroscopy (Horiba Jobin Yvon, HR800, France); while the phases and microstructure of the products were identified by X-ray diffraction analysis (XRD; X-Pert ProMPDDY2094, PANalytical), X-ray photoelectron spectroscopy (XPS; Thermo Scientific K-Alpha, USA), and scanning electron microscopy (SEM, Ultra Plus-43-13, Zeiss, Germany).

3. Results and Discussion
3.1 Sodium-penetrated graphite characterization

It has been reported that a large amount of sodium occupying 5%–10% of the cathode block can be produced, and can penetrate into the carbon cathode blocks during aluminum electrolysis [14]. Although some researchers have suggested that sodium can react with carbon to form an intercalation compound (Na_xC) [15,16], most researchers believe that adsorption between the graphene layers and in spaces associated with lattice defects is the major mechanism for sodium uptake in the carbon cathode blocks, and that the sodium is still in the form of a metal. On the one hand, sodium adsorbed by carbon cathode blocks is difficult to observe by XRD and SEM. On the other hand, Raman spectroscopy is remarkably sensitive to highly-symmetric covalent bonds with little or no natural dipole moment [17, 18]. Carbon materials fit perfectly into this criterion, and thus Raman spectroscopy has been widely used to observe slight changes of a graphite structure. Figure 1 shows the Raman spectra of the original graphite and the sodium-penetrated graphite at 514 nm wavelength excitation. The Raman spectra of both samples
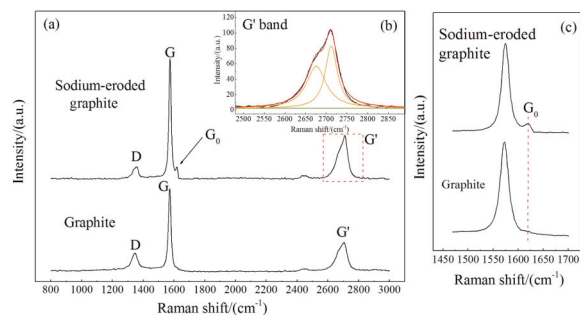
Figure 1. *Raman spectra of pristine graphite and sodium-penetrated graphite (a) entire Raman spectra of both samples, (b) G' band of sodium-penetrated graphite, (c) G_0 band of pristine and sodium-penetrated graphite*

contain three main bands that exhibit similar shapes and positions for both samples.

The G' band is caused by a double resonance process of the carbon atom, and is used to characterize the stacking mode between the graphite layers and the number of layers. Single-layer graphene is able to be fitted by one Lorentz peak. However, as the number of layers increases, the number of double resonance processes increases as well and the spectral shape converges to that of graphite where only two peaks are observed [19]. The G' band of the sodium-penetrated graphite sample, located at 2700 cm^{-1}, can be perfectly fitted by two Lorentz peaks and is identical with the graphite raw material (Fig. 1(b)). This indicates that the layer structure of graphite has not been destroyed during the reaction herein.

The D band at 1350 cm^{-1}, which arises from the vibration of the carbon lattice edge, indicates defects in the graphene sample. The ratio of the intensities of the G-band peak, I_G, and the D-band peak, I_D, is given as I_G/I_D; and is typically used as an indicator of the degree of graphitization. There is no D band in the Raman spectra of natural graphite.

The G band originates from the in-plane vibration of sp^2 carbon atoms [20], and thus was regarded herein as the graphene feature band. The so-called G band is frequently used to characterize hexagonal structures in the graphite lattice. Unlike the raw graphite spectra, the sodium-penetrated graphite exhibits a G_0 band at 1620 cm^{-1}, in addition to the G band (1575 cm^{-1}) that reveals the graphene structure. To manage graphite intercalation compounds, Nemanich and Solin have defined the Nearest Layer mode [21] that states that, the presence of two bands close to the G band location in Raman spectra are caused by the following two conditions: the first band (at 1575 cm^{-1} in Fig. 1(c)) is caused by the inner graphene at the center of the lattice that has less contact with sodium and still maintains obvious graphite features. The second blue-shifted G_0 band (at 1620 cm^{-1} in the sodium-penetrated graphite spectra of Fig. 1(c)) characterizes the 'outer' graphene layers bounded by intercalants [22]. The appearance of the G_0 band indicates that the intercalants have changed the graphite layer structure. In other words, the existence of the G_0 band in Raman spectra proved that the sodium and graphite produced sodium-graphite intercalation compounds (Na-GICs).

3.2 X-ray Photoemission Spectra (XPS) of Na-GICs

To obtain the existing state of Na and carbon elements in the intercalation compound, XPS was used to detect the Na-GICs, and the results are shown in Fig. 2.

Figure 2(a) shows a full-spectrum scan of the Na-GICs, where only the C1s peak is evident owing to the low content of sodium that makes the Na peak undetectable in the full spectra scan. Sodium and graphite can with great difficulty form stable lower-stage intercalation compounds like other alkali metals [23], and the content of intercalants in higher-stage intercalation compounds is much less than that in lower-stage compounds. The Na-GICs primarily are NaC$_{64}$, or even higher stages, and consequently there is a layer of sodium atoms every 64 or more layers of graphene in the Na-GICs. Thus, the content sodium in the Na-GICs is quite low. However, the Na1s peak can be detected by a detailed scan (Fig. 2(c)).

Curve-fitting of the C1s peak (Fig. 2(b)) reveals
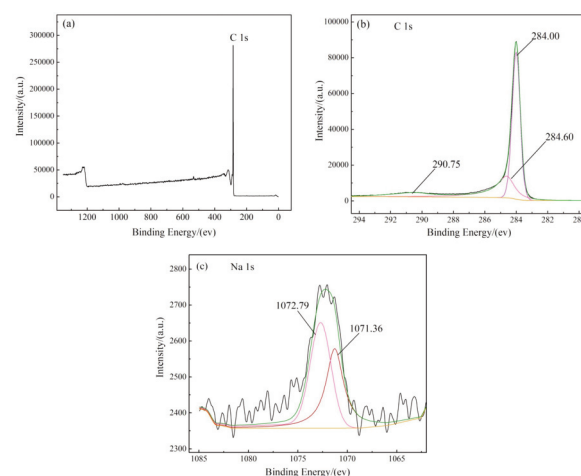
Figure 2. *XPS of the Na-GICs (a) full spectrum scan, (b) C 1s scan spectra, (c) Na 1s scan spectra*

that it comprises three peaks located at 284.00 (C$_1$), 284.58 (C$_2$), and 290.75 eV (C$_3$). The C$_2$ peak location corresponds to the pristine graphite peak value of 284.60 eV [24], indicating that the complete graphite structure remains intact after the reaction. The C$_1$ peak is located at a lower energy than the pristine graphite peak, indicating that charge is removed from the bonding states below the Fermi energy of graphite during the sodium reaction with graphite. The new Fermi edge is at lower energies with respect to the vacuum level, and thus the energy scale for photoemission is shifted to lower energies [25]. Finally, the C$_3$ peak may be owing to the C=O bond [26], indicating the presence of a graphite oxidation reaction.

Curve-fitting of the Na1s peak (Fig. 2(c)) reveals that the peak comprises two peaks, where the binding energy of the first is found to be 1,071.36 eV, which close to the Na1s characteristic peak location 1,071.40 eV [27]. The second peak at 1,072.79 eV may be owing to the oxidized sodium [28].

The XPS spectra show that some sodium is present in the graphite and that, during the reaction, sodium is inserted into the graphite layered structure as an intercalation agent.

3.3 SEM of graphite and Na-GICs
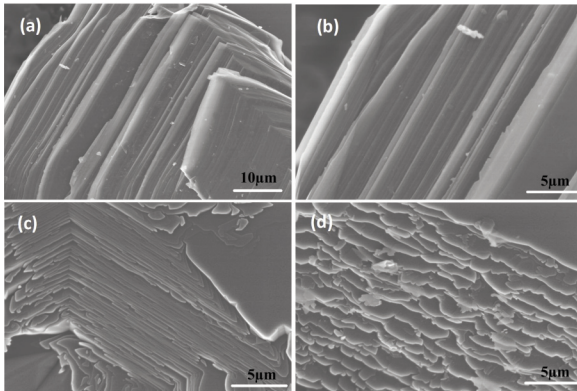
Figure 3. Surface morphology of the graphite layer structure (a and b) and Na-GICs (c and d)

Figure 3 shows SEM images of the pristine graphite and the Na-GICs, where numerous adjacent graphene layers are observed tightly stacked together to form many thick graphite blocks in the pristine graphite (Figs. 3(a) and 3(b)). The graphite blocks are arranged stepwise and the edges can be observed as smooth and tidy. The Na-GICs exhibit a layer structure with similar layer thickness as the pristine graphite (Figs. 3(c) and 3(d)), but the volume of the graphite is obviously expanded and the graphite blocks previously existing have disappeared. Further, the adjacent graphene layers are widely separated from each other, their edges are irregular, and the specific surface area increases substantially.

3.4 Characterization of products formed by aluminum/Na-GICs reaction

Analysis of the products obtained by the reaction between the Na-GICs and aluminum powder were obtained by XRD and SEM-EDS, and are respectively shown in Figs. 4 and 5.

It can be seen in Figs. 4 and 5 that C, Al_4C_3, and Al are the main phases of the final product. Therefore, aluminum can react with the Na-GICs to form Al_4C_3, but no Al_4C_3 can be found when aluminum reacts with
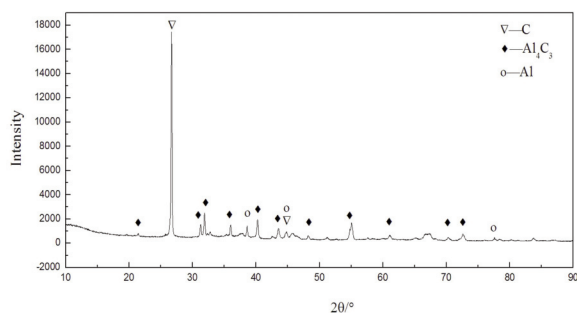
Figure 4. X-ray diffraction patterns of the reaction between Na-GICs and Al
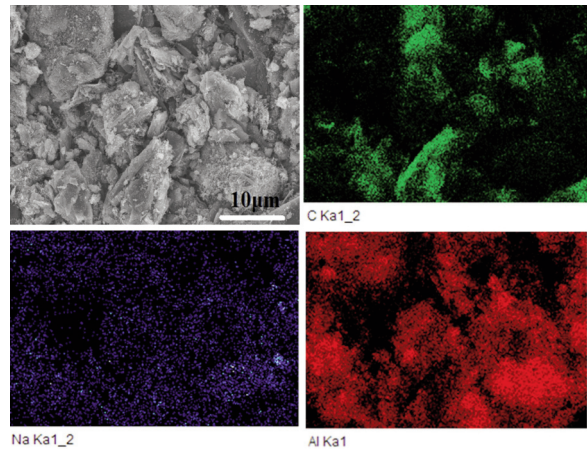
Figure 5. SEM and elements distribution of the final product

graphite in the same conditions. This result indicates that sodium has a decisive effect in the forming process of Al_4C_3, where the intercalation reaction changes the original graphite layered structure and thus changes the properties of the graphite. On the one hand, the graphite can expand in volume and effectively increase the contact area between graphite and aluminum. On the other hand, the sodium metal can destroy the oxide film on the surface of molten aluminum (Eq. 6), as given by

$$Al_2O_3 + 3Na = Al + 3Na_2O \qquad (6)$$
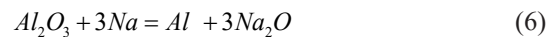
which increases the wettability of the aluminum-graphite system and promotes the reaction.

The generated reaction of Al_4C_3 can also proceed in the presence of NaF and aluminum because NaF easily reacts with aluminum to form metal sodium (Eqs. 7 and 8) when temperatures exceed 900°C [29-31], as given by

$$Al + 3NaF = AlF_3 + 3Na \qquad (7)$$

$$Al(l) + 6NaF(s) = Na_3AlF_6(s) + 3Na(s) \qquad (8)$$

The AlF_3 is involved in the follow-up response and the sodium reacts with graphite to form Na-GICs.

When cryolite is present, aluminum cannot react with the cryolite to form metal sodium at aluminum electrolysis temperatures, so Na-GICs cannot be generated. The action of cryolite is likely to serve as a wetting agent and as a solvent of the oxide films, but it is difficult to produce Al_4C_3 when the temperature is lower than 960°C.

4. Conclusions

(1) Graphite can react with metal sodium to form sodium-graphite intercalation compounds, which were detected by Raman spectroscopy. Sodium was

inserted into the graphite layered structure as an intercalation agent and still existed in a metal state in the compounds as well.

(2) The intercalation of sodium changed the original graphite layered structure by increasing the graphite volume and the specific surface area. Further, Al_4C_3 was produced by reacting the sodium-graphite intercalation compounds and aluminum. The presence of Na thus plays an important role in the formation process of Al_4C_3 in aluminum electrolysis cells.

Acknowledgements

References

[1] B. Novak, K. Tschöpe, A.P. Ratvik, T. Grande, Light metals, March 11-15, Orlando, USA, 2012, p.1343-1348.

[2] K. Vasshaug, T. Foosnæs, G.M. Haarberg, A.P. Ratvik, E. Skybakmoen, Light metals, February 15-19, San Francisco, USA, 2009, p. 1111-1116.

[3] X. Liao, H.A Øye, Light metals, February 15-19, San Antonio, USA, 1998, p. 667-674.

[4] W.L. Worell, Can. Metall. Quart., 4(1)(1964) 87-95.

[5] N.X. Feng, Aluminium Electrolysis, Chemical Industry Press of China, 2006, p. 128.

[6] M. Sørlie, H.A. Øye, Cathodes in Aluminum Electrolysis, Springer-Verlag GmbH-Heidelberg of Germany, 2010, P.215-217.

[7] R. C. Dorward, Metall. Trans. A, 4(1973) 386-388.

[8] P. Bonadia, F.A.O. Valenzuel, L.R. Bittencourt, Am. Ceram. Soc. Bull., 84(2) (2005) 26-30.

[9] A. Solheim, C. Schøning, E. Skybakmoen, Light Metals, February 14-18, Seattle, USA, 2010, p. 877-882.

[10] P.C. Hao. Reaction Mechanism of Dry Barrier Material of Aluminum Reduction Cell. PhD thesis. Northeastern University, Shenyang, China, 2018.

[11] J. Li, J. Fang, Q.Y. Li, Y.Q. Lai, J. Cent. South. Univ., 11(4)(2004)200-204.

[12] Z. Fang, X. Wu, J. Yu, L. Li, J.T. Zhu, Nonferr. Metal. Soc., 24(4)(2014) 1220-1230.

[13] Z. Fang, K. Zhang, X. Lv, L.B. Li, J. Zhu, J. Li, Nonferr. Metal. Soc., 23(6) (2013)1847−1853.

[14] Y.W. Wang, J.P. Peng, Y.Z. Di. JOM. 70(4)(2018) 1877-1883.

[15] C. Schøning, T. Grande, O.J. Siljan, Light Metals, February 28-March 4, 1999, San Diego, USA, 1999, p.849-856.

[16] O.J. Siljan, C Schoning, T Grande. JOM. 54 (5) (2002) 46-55.

[17] Y. Miyata, K. Mizuno, H. Kataura, J. Nanomater., 2011(2011) 1-7.

[18] M. Kakihana, M. Osada. Carbon Alloys. Elsevier Science. 2003, p.285-298.

[19] M.S. Dresselhaus, A. Jorio, M. Hofmann, G. Dresselhaus, R. Saito, Nano Lett., 10(3)(2010) 751-758.

[20] Z.H. Ni, Y.Y. Wang, T. Yu, Z.X. Shen, Nano Res., (4)(2008) 273-291.

[21] R.J. Nemanich, S.A. Solin, D. Gúerard, Phys. Rev. B., 16(6)(1977) 2665-2672.

[22] J.C. Chacón-Torres, L. Wirtz, T. Pichler, Phys. Status. Solidi-R., 251(12)(2015) 2337-2355.

[23] M. Hiroki, K. Akihide, C.A.J. Fisher, I. Yuichi, Rsc. Adv., 7(58)(2017) 36550-36554.

[24] J.Q. Wang, Introduction of Electronic Energy Spectrum (XPS/XAES/UPS). National Defence Industry Press of China, 1992, p.47-57.

[25] Y. Zhang, Z.X. Zhang, T.B Li, X.G. Liu, B.S. Xu, Spectrochim. Acta. A., 70(5)(2008) 1060-1064.

[26] G. Illing, D. Heskett, E.W. Plummer, H.J. Freund, Surf. Sci., 206 (1)(1988)1-19.

[27] S.P. Kowalczyk, L. Ley, F.R. McFeely, R.A. Pollak, D.A. Shirley, Phys. Rev. B., 8(8)(1973) 3583-3585.

[28] A. Barrie, F.J. Street, J. Electron. Spectrosc., 7(1)(1975) l-31.

[29] A.M. Pogodaeva, A.V. Proshkinb, P.V. Polyakov, Russ. J. Non-Ferr. Met., 51(4)(2010) 279-284.

[30] Y. Patrakhin, A.M. Pogodaev, A.V. Proshkin, P.V. Polyakov, I.A. Yarosh, R.V. Osipov, Refract. Ind. Ceram., 47(3)(2006) 183-188.

[31] A.V. Proshkin, A.M. Pogodaev, P.V. Polyakov, V.V. Pingin, I.A. Yarosh, Refract. Ind. Ceram., 49(2)(2008) 84-89.

Y.-W. Wang et al. / J. Min. Metall. Sect. B-Metall., 56 (3) (2020) 321 - 326

326

MEHANIZAM FORMIRANJA ALUMINIJUM KARBIDA U ĆELIJAMA ZA ELEKTROLIZU ALUMINIJUMA

Y.-W. Wang *, P.-C. Hao, J.-P. Peng, Y.-Z. Di

Metalurški fakultet, Severnoistočni univerzitet, Šenjang, Ljaoning, Kina

Apstrakt

Formiranje i rastvaranje aluminijum karbida se smatra primarnim faktorom koji utiče na životni vek ćelija za elektrolizu aluminijuma. U ovom radu su izmerene karakteristike natrijum-grafitnog interkalacionog jedinjenja (Na-GICs) i eksperimetalno je proučen mehanizam formiranja Al_4C_3 tokom postupka elektrolize aluminijuma. Ramanova spektroskopija, difrakcija x-zraka, fotoelektronska spektroskopija x-zraka i skenirajuća elektronska mikroskopija su metode korišćene za ispitivanje karakteristika Na-GIC i proizvoda reakcije aluminijuma i Na-GIC. Rezultati su pokazali da grafit reaguje sa metalom natrijuma i da se na taj način stvara jedinjenje Na-GIC koje može da se detektuje tehnikom Ramanove spektroskopije. Natrijum koji je ubačen u grafitnu slojevitu strukturu deluje kao sredstvo za interkalaciju koje menja originalnu grafitnu slojevitu strukturu i povećava zapreminu i specifičnu površinu grafita. Povrh toga, korišćenjem natrijum-grafitnog interkalacionog jedinjenja i aluminijuma kao materijala dobijen je Al_4C_3. Stoga, prisustvo natrijuma ima važnu ulogu u postupku formiranja Al_4C_3 u ćelijama za elektrolizu aluminijuma.

Ključne reči: Aluminjum karbid; Ćelije za elektrolizu aluminijuma; Prodiranje natrijuma; Grafit; Mehanizam formiranja